Final Technical Report

SISGR: Ultrafast Molecular Scale Chemical Imaging

Awardee Institution:
Northwestern University
633 Clark Street, Evanston, IL 60208-1110

Lead Principal Investigator:
Prof. Mark C. Hersam
Department of Materials Science and Engineering
Northwestern University
2220 Campus Drive, Evanston, IL 60208-3108
Phone: 847-491-2696; Fax: 847-491-7820
E-mail: m-hersam@northwestern.edu

Co-Princpal Investigators:
Dr. Jeffrey R. Guest (Argonne National Laboratory)
Dr. Nathan P. Guisinger (Argonne National Laboratory)
Dr. Saw Wai Hla (Argonne National Laboratory)
Prof. George C. Schatz (Northwestern University)
Prof. Tamar Seideman (Northwestern University)
Prof. Richard P. Van Duyne (Northwestern University)

Administrative Point of Contact:
Ms. Kelly Morrison
Executive Director, Office for Sponsored Research
Northwestern University
1801 Maple Ave., Suite 2410, Evanston, IL 60201-3149
Phone: 847-491-3003; Fax: 847-491-4800
E-mail: OSR-Evanston@northwestern.edu

DOE Office of Science Program Office:
Condensed Phase and Interfacial Science (CPIMS)

DOE Office of Science Program Office Technical Contact:
Dr. Gregory Fiechtner
E-mail: gregory.fiechtner@science.doe.gov

DOE Award Number:
DE-FG02-09ER16109

1. Overview

The Northwestern-Argonne SISGR program (DOE Grant Number DE-FG02-09ER16109) utilized newly developed instrumentation and techniques including integrated ultra-high vacuum tip-enhanced Raman spectroscopy/scanning tunneling microscopy (UHV-TERS/STM) and surface-enhanced femtosecond stimulated Raman scattering (SE-FSRS) to advance the spatial and temporal resolution of chemical imaging for the study of photoinduced dynamics of molecules on plasmonically active surfaces. An accompanying theory program addressed modeling of charge transfer processes using constrained density functional theory (DFT) in addition to modeling of SE-FSRS, thereby providing a detailed description of the excited state dynamics. This interdisciplinary and highly collaborative research resulted in 62 publications with ~ 48% of them being co-authored by multiple SISGR team members [1-62]. A summary of the scientific accomplishments from this SISGR program is provided in the following sections.

2. Ultrafast Tip-Enhanced Raman Spectroscopy

A primary goal of this SISGR program was the development of tools and techniques that enable ultrafast tip-enhanced Raman spectroscopy with single molecule sensitivity. Toward this end, progress was made in several areas:

(1) Ultrahigh vacuum (UHV) tip-enhanced Raman spectroscopy (TERS) integrated with molecular-resolution UHV scanning tunneling microscopy (STM). The first experimental accomplishment was the observation of multiple vibrational modes of copper phthalocyanine (CuPc) adlayers on Ag(111) using UHV-TERS with concurrently obtained sub-nanometer molecular-resolution STM imaging [2]. The observed vibrational modes agree well with density functional theory (DFT) calculations, thus confirming the quantitative nature of these measurements. The combination of molecular-resolution UHV-STM imaging with the detailed chemical information content of UHV-TERS allows the interactions between large polyatomic molecular adsorbates and specific binding sites on solid surfaces to be probed with unprecedented spatial and spectroscopic resolution.

(2) Low-temperature (LT) UHV-TERS. Low-temperature (19 K) UHV-TERS was also accomplished on the Rhodamine 6G (R6G)/Ag(111) system (**Figure 1**) [28]. In general, liquid He cooling minimizes surface diffusion of adsorbates across solid surfaces. LT-TER spectra differ from room-temperature (RT) TER, RT surface-enhanced Raman (SER), and LT-SER spectra because the vibrational lines are narrowed, due to decreased inhomogeneous broadening, and shifted, revealing additional chemical information about the adsorbate-substrate interactions. As an example, LT-TER spectra for the R6G/Ag(111) system are shown in **Figure 1** that exhibit such unique spectral shifts. Specifically, the orientation of R6G on Ag(111) was determined and corroborated by time-dependent density-functional theory (TDDFT) calculations. LT-TERS has thus been

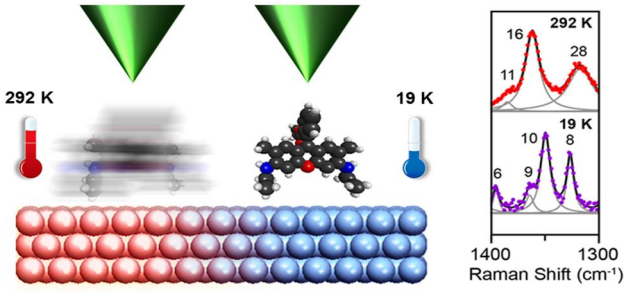

Figure 1. R6G surface diffusion is suppressed at 19 K. Its adsorption geometry on Ag(111) is characterized using low-temperature UHV-TERS, which exhibits line narrowing and peak shifts compared to room temperature UHV-TERS [28].

demonstrated as an effective approach for unraveling the intricacies of adsorbate-substrate interactions that are inaccessible by other means.

(3) TERS with pulsed laser excitation. In order to obtain kinetic information on the nanosecond to femtosecond timescales, pulsed laser excitation must be used. This goal was achieved by coupling picosecond-pulsed excitation from an optical parametric oscillator (OPO) to an ambient STM, where TERS was observed for two resonant analytes on a silver film [29]. The signal irreversibly degraded on the timescale of tens of seconds, which was not a result of tip damage. An analysis of the decay kinetics using models for various physical processes revealed reactive decay chemistry and photothermal desorption as the dominant degradation mechanisms in ambient conditions. Analogous experiments were then performed in UHV to minimize reactive decay between excited analytes and small molecules present in ambient [30]. Picosecond excitation from the OPO was coupled to our UHV STM, and the resulting pulsed UHV-TER spectra were multimodal and similar in character to CW TER spectra. The signal was observed to fluctuate in intensity over time but not irreversibly degrade. In picosecond SERS, in which intensity fluctuations are not observed, the signal was found to be slowed by a factor of ~5 in UHV compared to in ambient. Analysis of the picosecond SER signal decay revealed surface diffusion as the most likely responsible mechanism. By mitigating degradation pathways, these results demonstrate that a UHV environment is a valuable asset for time-resolved TERS studies.

(4) Analysis of the relative intensity fluctuations observed in SMTERS. The origin of relative intensity fluctuations among peaks in single-molecule (SM) TERS has been a long-standing question in the field. The combination of SMTERS and TDDFT results provided insight into the potential causes of these fluctuations [21]. Molecular orientation and field gradient effects could not explain the phenomena observed in experimental SMTER spectra, but the fluctuations were computationally reproducible by allowing small variations (< 20%) in the excited-state geometry. These variations in excited-state properties reveal detailed information about adsorbate-adsorbate and/or adsorbate-surface interactions.

3. Chemically Modified Graphene and Silicon on Plasmonic Substrates

To diversify the substrates and surface chemistries compatible with ultrafast UHV-TERS/STM measurements, the SISGR team developed atomically thin crystalline graphene and silicon coatings on plasmonically active silver and gold surfaces. Furthermore, extensive *in situ* chemical functionalization methods on graphene and silicon were developed. Principal research accomplishments in this theme include:

(1) UHV growth of graphene on Ag(111). The SISGR team demonstrated the first growth of graphene on plasmonically active Ag(111) surfaces [18], which had been a challenge to the scientific community because of the inert nature of Ag. Since traditional chemical vapor deposition (CVD) techniques that are typically utilized for graphene growth are ineffective on Ag substrates, an alternative method based on

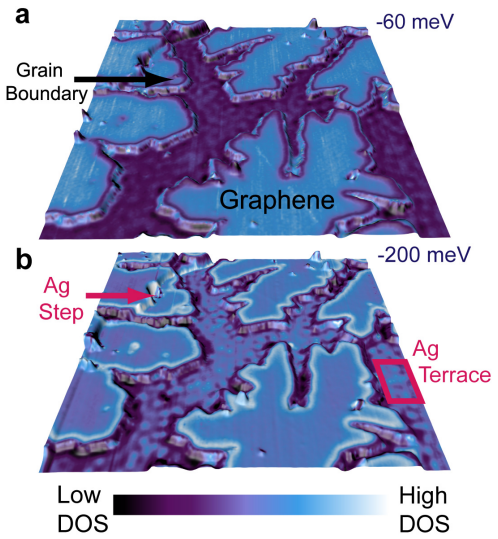

Figure 2. Spatially resolved differential tunneling conductance imaging reveals electron scattering at the edges of graphene grown on Ag(111). Image sizes are both 150 nm x 150 nm [18].

direct deposition of elemental carbon (i.e., carbon evaporated from a graphite rod via e-beam heating) was developed. The resulting graphene grown on Ag(111) is highly decoupled from the surface and exhibits electron scattering from its edges at the Fermi wavelength (**Figure 2**), which is the first such observation for graphene on any metallic substrate.

(2) Graphene nanoribbons on Au(111). In addition to bulk graphene, progress was made on the growth of graphene nanoribbons on plasmonically active Au(111) surfaces. Specifically, halogenated polycyclic aromatic hydrocarbons allowed graphene nanoribbons to be formed via ring-coupling reactions on Au(111). At the initial stage, the molecules self-assemble to form a noncovalently interacting adlayer. However, after annealing the substrate to 500 K, the molecules covalently cross-link via scission of the halogen bonds. Further annealing of the substrate to 750 K finally results in the formation of graphene nanoribbons. The structural and electronic properties of the graphene nanoribbons were investigated at the single nanoribbon level using STM and scanning tunneling spectroscopy, respectively.

(3) Two-dimensional silicon growth on Ag(111). In an effort to diversify the range of surface chemistries on plasmonically active substrates, the SISGR team also completed an extensive study that followed the evolution of silicon deposition on Ag(111) from multiple surface alloy phases to the precipitation of two-dimensional sheets of sp^3-bonded silicon [27]. This silicon growth method is compatible with graphene growth on silver, thus allowing the synthesis of both lateral and vertical graphene-silicon heterostructures. These substrates thus allow direct interrogation of the interaction of adsorbates with two contrasting surfaces: highly reactive silicon and relatively inert graphene, which tend to interact with adsorbates in a covalent and noncovalent manner, respectively.

(4) Chemical functionalization of graphene and silicon. In addition to graphene growth on plasmonic substrates, methods for chemically functionalizing graphene and silicon were concurrently developed. For example, the SISGR team achieved the formation of well-defined one-dimensional organic nanostructures on graphene via the self-assembly of 10,12 pentacosadiynoic acid (PCDA) in UHV [1]. Molecular resolution UHV STM images confirm the one-dimensional ordering of the as-deposited PCDA monolayer and show domain boundaries with symmetry consistent with the underlying graphene lattice. These PCDA monolayers were then utilized as templates for atomic layer deposition (ALD) of diethyl zinc, resulting in ordered ZnO nanowires on graphene with sub-10 nm widths [25]. In addition, atomic oxygen exposure in UHV allowed chemically homogeneous and reversible epoxidation of graphene [12] that modulates the electronic

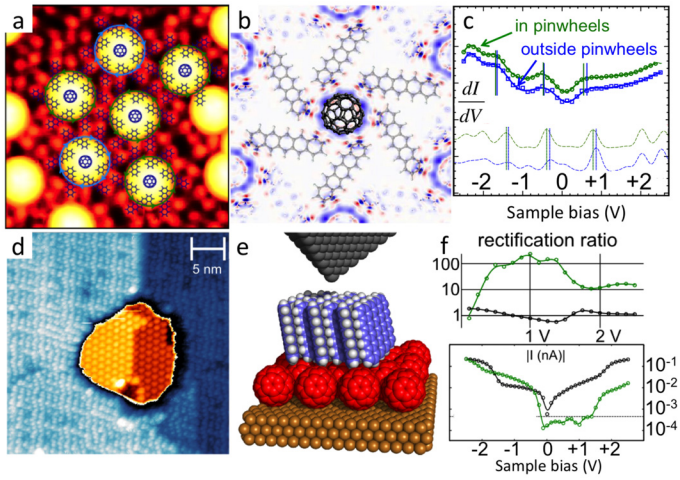

Figure 3. Pn-C_{60} heterojunctions. (a) STM image overlaid with model of chiral heterojunctions. (b) Charge difference calculation showing electron transfer (blue) to C_{60}. (c) STS (top) and calculated local density of states (bottom) for Pn in (green) and outside (blue) chiral heterojunctions. (d) STM image and (e) model of a Pn/C_{60}/Cu stacked heterojunction. (f) Transport and rectification ratio over the heterojunction (green) and over C_{60} alone (black) [13].

and chemical properties of the underlying graphene [22]. Subsequent *in situ* exposure of graphene epoxide to ALD precursors resulted in the growth of metal oxide nanoparticles, which were characterized experimentally with STM, X-ray photoelectron spectroscopy, and Raman spectroscopy, and modeled atomistically with DFT [15]. Additional chemical functionalization strategies were also demonstrated including covalent modification of silicon with cyclopentene [24], aqueous-phase oxidation of graphene [36], and noncovalent organic assemblies of perylenetetracarboxylic diimide (PTCDI) [37] and melamine [38] on graphene.

4. Molecular Heterojunctions

Donor-acceptor molecular heterojunctions are at the heart of organic photovoltaic and optoelectronic processes because they provide the intrinsic electric fields that separate photogenerated charges. Since their electronic properties and photophysical behavior hinge on local morphology down to the atomic scale, molecular heterojunctions were fabricated and characterized with UHV STM:

(1) Self-assembled in-plane chiral heterojunctions between small molecule acceptors and donors. Pentacene (Pn) and C_{60} – archetypal donor and acceptor molecules – were self-assembled into in-plane heterojunctions Cu(111) surfaces as shown in the UHV STM image in **Figure 3a**. Unexpectedly, these highly symmetric molecules form *chiral* heterojunctions, providing a striking demonstration of symmetry-breaking through self-assembly of molecules on a surface [13]. Using scanning tunneling spectroscopy (STS), the signature shifts of the energy levels of the Pn molecules were resolved in these heterojunctions. The resulting evidence of charge transfer between the Pn and C_{60} show that these structures are functional donor-acceptor heterojunctions (**Figure 3b**). Comparing these measurements with DFT confirms that these chiral structures are energetically favored and determines the amount of charge transfer between the Pn and C_{60} in these heterojunctions (**Figure 3c**).

(2) Rectification through stacked molecular heterojunctions. Stacked donor-acceptor heterojunctions on Cu(111) were self-assembled in both orientations (Pn/C_{60}/Cu and C_{60}/Pn/Cu) in order to measure and understand transport through these heterojunction systems. By depositing a monolayer of C_{60} on Cu(111) followed by a submonolayer of Pn, a two-molecule-thick donor-acceptor rectifier was realized as imaged in **Figure 3d** and modeled in **Figure 3e**. Current-voltage curves (**Figure 3f**) taken over the heterojunction (green), which show strong rectification, contrast sharply with the curves taken over C_{60} alone (black), which are nearly symmetric. Rectification ratios between forward and reverse bias currents exceed 100x in this two-molecule thick geometry. The opposite orientation also revealed rectification, albeit weaker, in the reverse direction. DFT calculations confirm the large rectification ratio in the Pn/C_{60}/Cu orientation and show that the metallic nature of C_{60} on Cu plays a critical role in realizing favorable level alignment for rectification.

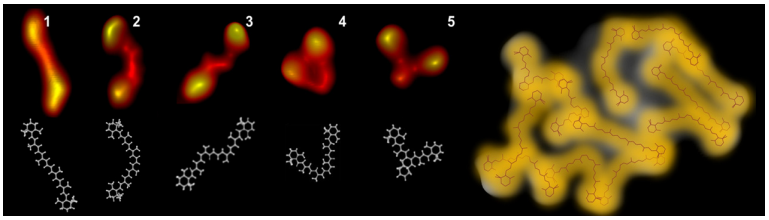

Figure 4. Five β-carotene conformations (left) and β-carotene complex (right) as revealed by UHV STM.

5. Single Molecule Characterization and Manipulation

In addition to molecular assemblies, the SISGR team pursued UHV STM characterization down to the single molecule limit at cryogenic temperatures. This work also included single

molecular manipulation experiments, which allow atomically precise geometries to be realized and also reveal the fundamentals of molecule-substrate interactions. Specific accomplishments include:

(1) STM manipulation of photosynthetic plant molecular complexes. β-carotene and chlorophyll-a are vital molecules for the existence of life on Earth, but their detailed structures in molecular complexes had not previously been investigated at single molecule level. Using single molecule manipulation schemes, the detailed molecular structures of β-carotene and chlorophyll-a were resolved in molecular complexes at sub-molecular resolution (**Figure 4**). Five β-carotene conformations were imaged for the first time, and their structural integrity was tested by STM manipulation. These experiments reveal that β-carotene destroys ordered chlorophyll-a clusters to form molecular complexes where the two different molecular species tend to position next to each other. Moreover, evidence of inducing chlorophyll-a conformational changes by β-carotene was found, thereby revealing their preferential interactions that enhance charge and energy transfer processes at the molecular scale.

(2) Nanoscale molecule-cavity complexes. STM tip manipulation schemes were used to create polyatomic nano cavities on the plasmonic surface of Ag(111), and then determine the resulting electronic structures locally for the first time. In particular, the variation of local surface potential and the energetic positions of resonances were observed while in the field emission regime. These experiments revealed the existence of distinct electronic states in these cavities above the surface Fermi level. Furthermore, the influence of these cavities on the electronic structure of TBrPP-Co molecules was determined by inserting individual molecules into the cavities using STM manipulation. Spectroscopic data exhibit significant shifts of the measured molecular orbitals when compared to molecules on the clean surface. The observed changes are attributable to the altered local potential above the cavities compared to the clean surface terraces.

(3) Lateral force needed to move a single molecule on graphene nanoribbons. A molecular-scale study of the lateral force required to move a single molecule on graphene was performed. Specifically, diffusion of TBrPP-Co molecules on graphene nanoribbons was controlled by STM manipulation along the long graphene nanoribbon axis (**Figure 5**). From the manipulation signals, the force was quantified as function of the tip-height. From the linear dependence of the force angle on tip-height, the slope of the attractive tip-molecule force was deduced. These measurements show that piconewton-scale lateral forces are required to move individual TBrPP-Co molecules on graphene nanoribbons.

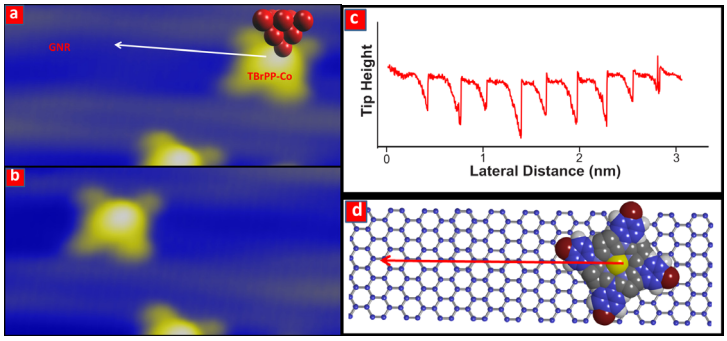

Figure 5. (a,b) A TBrPP-Co molecule is laterally moved along the long axis of a graphene nanoribbon via STM tip manipulation. (c) The corresponding STM tip manipulation signal. (d) A model illustrates the TBrPP-Co manipulation on a graphene nanoribbon.

6. References

[1] A. Deshpande, C.-H. Sham, J. M. P. Alaboson, J. M. Mullin, G. C. Schatz, and M. C. Hersam, "Self-assembly and photopolymerization of sub-2 nm one-dimensional organic nanostructures on graphene," *J. Am. Chem. Soc.*, **134**, 16759 (2012).

[2] N. Jiang, E. T. Foley, J. M. Klingsporn, M. D. Sonntag, N. A. Valley, J. A. Dieringer, T. Seideman, G. C. Schatz, M. C. Hersam, and R. P. Van Duyne, "Observation of multiple vibrational modes in ultrahigh vacuum tip-enhanced Raman spectroscopy combined with molecular-resolution scanning tunneling microscopy," *Nano Lett.*, **12**, 5061 (2012).

[3] J. Mullin, N. Valley, M. G. Blaber, and G. C. Schatz, "Combined quantum mechanics (TDDFT) and classical electrodynamics (Mie theory) methods for calculating surface enhanced Raman and hyper-Raman spectra," *J. Phys. Chem. A*, **116**, 9574 (2012).

[4] J. Mullin and G. C. Schatz, "A combined linear response quantum mechanics and classical electrodynamics (QM/ED) method for the calculation of surface enhanced Raman spectra," *J. Phys. Chem. A*, **116**, 1931 (2012).

[5] J. M. Mullin, J. Autschbach, and G. C. Schatz, "Time-dependent density functional methods for surface enhance Raman scattering (SERS) studies," *Comp. Theor. Chem.*, **987**, 32 (2012).

[6] R.R. Frontiera, N. L. Gruenke, and R. P. Van Duyne, "Fano-like resonances arising from long-lived molecule-plasmon interactions in colloidal nanoantennas," *Nano. Lett.*, **12**, 5989 (2012).

[7] B. Sharma, R. R. Frontiera, A.-I. Henry, E. Ringe, and R. P. Van Duyne, "SERS: Materials, applications, and the future," *Mater. Today*, **15**, 16 (2012).

[8] A. Salomon, R. J. Gordon, Y. Prior, T. Seideman, and M. Sukharev, "Strong coupling between molecular excited states and surface plasmon modes of a slit array in a thin metal film," *Phys. Rev. Lett.*, **109**, 073002 (2012).

[9] M. G. Reuter, M. A. Ratner, and T. Seideman, "Laser alignment as a route to ultrafast control of electron transport through junctions," *Phys. Rev. A*, **86**, 013426 (2012).

[10] M. G. Reuter, M. C. Hersam, T. Seideman, and M. A. Ratner, "Signatures of cooperative effects and transport mechanisms in conductance histograms," *Nano Lett.*, **12**, 2243 (2012).

[11] J. Cho, J. Smerdon, L. Gao, Ö. Süzer, J. R. Guest, and N. P. Guisinger, "Structural and electronic decoupling of C_{60} from Epitaxial Graphene on SiC," *Nano Lett.*, **12**, 3018 (2012).

[12] Md. Z. Hossain, J. E. Johns, K. H. Bevan, H. J. Karmel, Y. T. Liang, S. Yoshimoto, K. Mukai, T. Koitaya, J. Yoshinobu, M. Kawai, A. M. Lear, L. L. Kesmodel, S. L. Tait, and M. C. Hersam, "Chemically homogeneous and thermally reversible oxidation of epitaxial graphene," *Nature Chemistry*, **4**, 305 (2012).

[13] J. A. Smerdon, N. P. Guisinger, and J. R. Guest, "Chiral 'pinwheel' heterostructure self-assembled from C_{60} and pentacene," *ACS Nano*, **7**, 3086 (2013).

[14] N. Valley, N. Greeneltch, R. P. Van Duyne, and G. C. Schatz, "A look at the origin and magnitude of the chemical contribution to the enhancement mechanism of surface-enhanced Raman spectroscopy (SERS): theory and experiment," *J. Phys. Chem. Lett.*, **4**, 2599 (2013).

[15] J. E. Johns, J. M. P. Alaboson, S. Patwardhan, C. R. Ryder, G. C. Schatz, and M. C. Hersam, "Metal oxide nanoparticle growth on graphene via chemical activation with atomic oxygen," *J. Am. Chem. Soc.*, **135**, 18121 (2013).

[16] E. Yitamben, R. B. Rankin, E. V. Iski, J. P. Greeley, R. A. Rosenberg, and N. P. Guisinger, "Tracking molecular motion in quantum corals," *J. Phys. Chem. C*, **117**, 11757 (2013).

[17] E. V. Iski, E. N. Yitamben, L. Gao, and N. P. Guisinger, "Graphene at the atomic-scale: synthesis, characterization and modification," *Adv. Funct. Mat.*, **23**, 2554 (2013).

[18] B. Kiraly, E. V. Iski, A. J. Mannix, M. C. Hersam, and N. P. Guisinger, "Solid-source growth and atomic-scale characterization of graphene on Ag(111)," *Nat. Comm.*, **4**, 2804 (2013).

[19] S. Kleinman, R. R. Frontiera, A.-I. Henry, J. A. Dieringer, and R. P. Van Duyne, "Creating, characterizing, and controlling chemistry with SERS hot spots," *Phys. Chem. Chem. Phys.*, **15**, 21 (2013).

[20] E. Pozzi, M. Sonntag, N. Jiang, J. Klingsporn, M. C. Hersam, and R. P. Van Duyne, "Tip-enhanced Raman imaging: An emergent tool for probing biology at the nanoscale," *ACS Nano*, **7**, 885 (2013).

[21] M. D. Sonntag, D. Chulhai, T. Seideman, L. Jensen, and R. P. Van Duyne, "The origin of relative intensity fluctuations in single-molecule tip-enhanced Raman spectroscopy," *J. Am. Chem. Soc.,* **135**, 17187 (2013).

[22] A. Natan, M. C. Hersam, and T. Seideman, "Insights into graphene functionalization by single atom doping," *Nanotech.*, **24**, 505715 (2013).

[23] M. Kornbluth, A. Nitzan, and T. Seideman, "Light-induced electronic non-equilibrium in plasmonic particles," *J. Chem. Phys.*, **138**, 174707 (2013).

[24] H. J. Karmel and M. C. Hersam, "Room temperature molecular resolution nanopatterning of cyclopentene monolayers on Si(100) via feedback controlled lithography," *Appl. Phys. Lett.*, **102**, 243106 (2013).

[25] J. M. P. Alaboson, C.-H. Sham, S. Kewalramani, J. D. Emery, J. E. Johns, A. Deshpande, T. Chien, M. J. Bedzyk, J. W. Elam, M. J. Pellin, and M. C. Hersam, "Templating sub-10 nm atomic layer deposited oxide nanostructures on graphene via one-dimensional organic self-assembled monolayers," *Nano Lett.*, **13**, 5763 (2013).

[26] F. W. Aquino and G. C. Schatz, "Time-dependent density functional methods for Raman spectra in open-shell systems," *J. Phys. Chem. A*, **118**, 517 (2014).

[27] A. J. Mannix, B. Kiraly, B. L. Fisher, M. C. Hersam, and N. P. Guisinger, "Silicon growth at the two-dimensional limit on Ag(111)," *ACS Nano*, **8**, 7538 (2014).

[28] J. M. Klingsporn, N. Jiang, E. A. Pozzi, M. D. Sonntag, D. Chulhai, T. Seideman, L. Jensen, M. C. Hersam, and R. P. Van Duyne, "Intramolecular insight into adsorbate-substrate interactions via low temperature, ultrahigh vacuum tip-enhanced Raman spectroscopy," *J. Am. Chem. Soc.,* **136**, 3881 (2014).

[29] J. M. Klingsporn, M. D. Sonntag, T. Seideman, and R. P. Van Duyne, "Tip-enhanced Raman spectroscopy with picosecond pulses," *J. Phys. Chem. Lett.,* **5**, 106 (2014).

[30] E. A. Pozzi, M. D. Sonntag, N. Jiang, N. Chiang, T. Seideman, M. C. Hersam, and R. P. Van Duyne, "Ultrahigh vacuum tip-enhanced Raman spectroscopy with picosecond excitation," *J. Phys. Chem. Lett.,* **5**, 2657 (2014).

[31] M. D. Sonntag, E. A. Pozzi, N. Jiang, M. C. Hersam, and R. P. Van Duyne, "Recent advances in tip-enhanced Raman spectroscopy," *J. Phys. Chem. Lett.,* **5**, 3125 (2014).

[32] S. M. Parker, M. Smeu, I. Franco, M. A. Ratner, and T. Seideman, "Molecular junctions: Can pulling influence optical controllability?" *Nano Lett.*, **14**, 4587 (2014).
[33] B. Feldman, T. Seideman, O. Hod, and L. Kronik, "Real-space method for highly parallelizable electronic transport calculations," *Phys. Rev. B*, **90**, 035445 (2014).
[34] A. Deinega and T. Seideman, "Self-interaction-free approaches for self-consistent solution of the Maxwell-Liouville equations," *Phys. Rev. A*, **89**, 022501 (2014).
[35] Z. Hu, M. A. Ratner, and T. Seideman, "Modeling light-induced charge transfer dynamics across a metal-molecule-metal junction: Bridging classical electrodynamics and quantum dynamics," *J. Chem. Phys.*, **141**, 224104 (2014).
[36] Md. Z. Hossain, M. B. A. Razak, S. Yoshimoto, K. Mukai, T. Koitaya, J. Yoshinobu, H. Sone, S. Hosaka, and M. C. Hersam, "Aqueous-phase oxidation of epitaxial graphene on the silicon face of SiC(0001)," *J. Phys. Chem. C*, **118**, 1014 (2014).
[37] H. J. Karmel, J. J. Garramone, J. D. Emery, S. Kewalramani, M. J. Bedzyk, and M. C. Hersam, "Self-assembled organic monolayers on epitaxial graphene with enhanced structural and thermal stability," *Chem. Comm.*, **50**, 8852 (2014).
[38] H. J. Karmel, T. Chien, V. Demers-Carpentier, J. J. Garramone, and M. C. Hersam, "Self-assembled two-dimensional heteromolecular nanoporous molecular arrays on epitaxial graphene," *J. Phys. Chem. Lett.*, **5**, 270 (2014).
[39] A. J. Shearer, J. E. Johns, B. W. Caplins, D. E. Suich, M. C. Hersam, and C. B. Harris, "Electron dynamics of the buffer layer and bilayer graphene on SiC," *Appl. Phys. Lett.*, **104**, 231604 (2014).
[40] J. D. Emery, V. H. Wheeler, J. E. Johns, M. E. McBriarty, B. Detlefs, M. C. Hersam, D. K. Gaskill, and M. J. Bedzyk, "Structural consequences of hydrogen intercalation of epitaxial graphene on SiC(0001)," *Appl. Phys. Lett.*, **105**, 161602 (2014).
[41] G. Li, B. D. Fainberg, and T. Seideman, "Optically induced transport through semiconductor-based molecular electronics," *J. Chem. Phys.*, **142**, 154111 (2015).
[42] M. B. Ross and G. C. Schatz, "Radiative effects in plasmonic aluminum and silver nanospheres and nanorods," *J. Phys. D: Appl. Phys.*, **48**, 184004 (2015).
[43] N. Chiang, N. Jiang, D. V. Chulhai, E. A. Pozzi, M. C. Hersam, L. Jensen, T. Seideman, and R. P. Van Duyne, "Molecular-resolution interrogation of a porphyrin monolayer by ultrahigh vacuum tip-enhanced Raman and fluorescence spectroscopy," *Nano Lett.*, **15**, 4114 (2015).
[44] R. M. Jacobberger, B. Kiraly, M. Fortin-Deschenes, P. L. Levesque, K. M. McElhinny, G. J. Brady, R. R. Delgado, S. S. Roy, A. Mannix, M. G. Lagally, P. G. Evans, P. Desjardins, R. Martel, M. C. Hersam, N. P. Guisinger, and M. S. Arnold, "Direct oriented growth of armchair graphene nanoribbons on germanium," *Nature Communications*, **6**, 8006 (2015).
[45] B. Kiraly, A. J. Mannix, M. C. Hersam, and N. P. Guisinger, "Graphene-silicon heterostructures at the two-dimensional limit," *Chem. Mater.*, **27**, 6085 (2015).
[46] E. A. Pozzi, A. B. Zrimsek, C. M. Lethiec, G. C. Schatz, M. C. Hersam, and R. P. Van Duyne, "Evaluating single-molecule Stokes and anti-Stokes SERS for nanoscale thermometry," *J. Phys. Chem. C*, **119**, 21116 (2015).
[47] B. Kiraly, R. M. Jacobberger, A. J. Mannix, G. P. Campbell, M. J. Bedzyk, M. S. Arnold, M. C. Hersam, and N. P. Guisinger, "Electronic and mechanical properties of graphene-germanium interfaces grown by chemical vapor deposition," *Nano Lett.*, **15**, 7414 (2015).

[48] P. P. Pal, N. Jiang, M. D. Sonntag, N. Chiang, E. T. Foley, M. C. Hersam, R. P. Van Duyne, and T. Seideman, "Plasmon-mediated electron transport in tip-enhanced Raman spectroscopic junctions," *J. Phys. Chem. Lett.*, **6**, 4210 (2015).

[49] A. J. Mannix, X.-F. Zhou, B. Kiraly, J. D. Wood, D. Alducin, B. D. Myers, X. Liu, B. L. Fisher, U. Santiago, J. R. Guest, M. J. Yacaman, A. Ponce, A. R. Oganov, M. C. Hersam, and N. P. Guisinger, "Synthesis of borophenes: Anisotropic, two-dimensional boron polymorphs," *Science*, **350**, 1513 (2015).

[50] X. Liu, I. Balla, H. Bergeron, G. P. Campbell, M. J. Bedzyk, and M. C. Hersam, "Rotationally commensurate growth of MoS_2 on epitaxial graphene," *ACS Nano*, **10**, 1067 (2016).

[51] L. Gao, P. P. Pal, T. Seideman, N. P. Guisinger, and J. R. Guest, "Current-driven hydrogen desorption from graphene: Experiment and theory," *J. Phys. Chem. Lett.*, **7**, 486 (2016).

[52] C. J. Tainter and G. C. Schatz, "Reactive force field modeling of zinc oxide nanoparticle formation," *J. Phys. Chem. C*, **120**, 2950 (2016).

[53] J. A. Smerdon, N. C. Giebink, N. P. Guisinger, P. Darancet, and J. R. Guest, "Large spatially resolved rectification in a donor-acceptor molecular heterojunction," *Nano Lett.*, **16**, 2603 (2016).

[54] M. B. Ross, J. C. Ku, B. Lee, C. A. Mirkin, and G. C. Schatz, "Plasmonic metallurgy enabled by DNA," *Adv. Mater.*, **28**, 2790 (2016).

[55] B. Kiraly, A. J. Mannix, R. M. Jacobberger, B. L. Fisher, M. S. Arnold, M. C. Hersam, and N. P. Guisinger, "Sub-5 nm, globally aligned graphene nanoribbons on Ge(001)," *Appl. Phys. Lett.*, **108**, 213101 (2016).

[56] C. R. Ryder, J. D. Wood, S. A. Wells, Y. Yang, D. Jariwala, T. J. Marks, G. C. Schatz, and M. C. Hersam, "Covalent functionalization and passivation of exfoliated black phosphorus via aryl diazonium chemistry," *Nature Chemistry*, **8**, 597 (2016).

[57] N. Jiang, N. Chiang, L. R. Madison, E. A. Pozzi, M. R. Wasielewski, T. Seideman, M. A. Ratner, M. C. Hersam, G. C. Schatz, and R. P. Van Duyne, "Nanoscale chemical imaging of a dynamic molecular phase boundary with ultrahigh vacuum tip-enhanced Raman spectroscopy," *Nano Lett.*, **16**, 3898 (2016).

[58] E. A. Pozzi, N. L. Gruenke, N. Chiang, D. V. Zhdanov, N. Jiang, T. Seideman, G. C. Schatz, M. C. Hersam, and R. P. Van Duyne, "Operational regimes in picosecond and femtosecond pulse-excited ultrahigh vacuum SERS," *J. Phys. Chem. Lett.*, **7**, 2971 (2016).

[59] N. Jiang, D. Kurouski, E. A. Pozzi, N. Chiang, M. C. Hersam, and R. P. Van Duyne, "Tip-enhanced Raman spectroscopy: From concepts to practical applications," *Chem. Phys. Lett.*, **659**, 16 (2016).

[60] X. Liu, I. Balla, H. Bergeron, and M. C. Hersam, "Point defects and grain boundaries in rotationally commensurate MoS_2 on epitaxial graphene," *J. Phys. Chem. C*, **120**, 20798 (2016).

[61] Z. Zhang, A. J. Mannix, Z. Hu, B. Kiraly, N. P. Guisinger, M. C. Hersam, and B. I. Yakobson, "Substrate-induced nanoscale undulations of borophene on silver," *Nano Lett.*, **16**, 6622 (2016).

[62] N. Chiang, X. Chen, G. Goubert, D. V. Chulhai, X. Chen, E. A. Pozzi, N. Jiang, M. C. Hersam, T. Seideman, L. Jensen, and R. P. Van Duyne, "Conformational contrast of surface-mediated molecular switches yields angstrom-scale spatial resolution in ultrahigh vacuum tip-enhanced Raman spectroscopy," *Nano Lett.*, **16**, 7774 (2016).